Wurtzite−Chalcopyrite Polytypism in $CuInS_2$ Nanodisks

Bonil Koo, Reken N. Patel, and Brian A. Korgel*

Department of Chemical Engineering, Texas Materials Institute, Center for Nano- and Molecular Science and Technology, The University of Texas at Austin, Austin, Texas 78712-1062

Received February 8, 2009. Revised Manuscript Received March 11, 2009

Monodisperse $CuInS_2$ nanodisks were synthesized by heating metal chlorides and thiourea in oleylamine. X-ray diffraction showed the predominant phase to be wurtzite (hexagonal) $CuInS_2$ instead of chalcopyrite (tetragonal) or compositionally disordered sphalerite (cubic). High-resolution transmission electron microscopy, however, revealed polytypism in the nanodisks, with the wurtzite phase interfaced with significant chalcopyrite domains.

Introduction

Solvent dispersions, or "inks", of nanocrystals of ternary I−III−VI_2 compounds like $CuInS_2$ have been the target of recent synthetic efforts because of their potential as light-absorbing materials in printed and flexible photovoltaic devices (PVs).[1−5] These materials have band gap energies near the red edge of the visible spectrum, high optical absorption coefficients, and durable photostability, and when deposited by vapor-phase routes, they have been used to achieve high efficiency (>10%) PVs.[6,7] Recent studies have demonstrated the incorporation of I−III−VI_2 nanocrystals into functioning PVs, although the power conversion efficiencies have been relatively low (<5%).[1−5] Part of the challenge facing these efforts has been the need for better synthetic methods for nanocrystals of the desired I−III−VI_2 compound.

$CuInS_2$ nanocrystals have been synthesized by a number of research groups in the recent past, but the chemistry continues to be refined to obtain nanocrystals with improved size control.[3,8−19] Here, we provide a new synthetic route to monodisperse $CuInS_2$ nanodisks. Recent examples of shape control have appeared for $CuInSe_2$ nanocrystals, including doughnuts[2] and trigonal pyramids,[20] but no similar examples of nonspherical nanocrystals of $CuInS_2$. X-ray diffraction (XRD) showed that the $CuInS_2$ nanodisks had wurtzite crystal structure instead of the expected tetragonal chalcopyrite phase[21] or com-

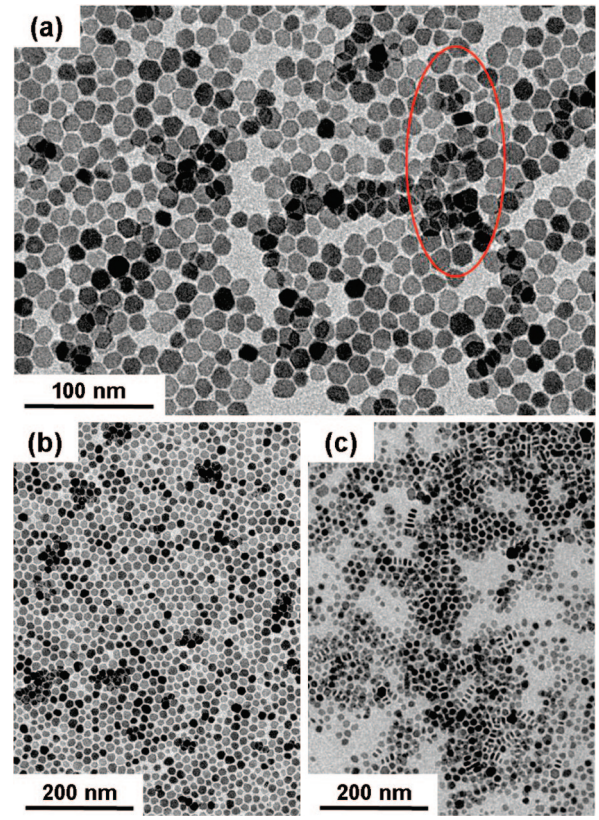

Figure 1. TEM images of $CuInS_2$ nanodisks. The dimensions are 13.4 ± 1.6 nm (diameter) and 5.7 ± 0.6 nm (thickness). The red oval in (a) highlights a region of nanodisks oriented on their sides and the image in (c) shows many nanodisks on their sides.

* Corresponding author. Tel.: 512-471-5633. Fax: 512-471-7060. E-mail: korgel@mail.che.utexas.edu.

(1) Panthani, M. G.; Akhavan, V.; Goodfellow, B.; Schmidtke, J. P.; Dunn, L.; Dodabalapur, A.; Barbara, P. F.; Korgel, B. A. *J. Am. Chem. Soc.* **2008**, *130*, 16770–16777.
(2) Guo, Q. J.; Kim, S. J.; Kar, M.; Shafarman, W. N.; Birkmire, R. W.; Stach, E. A.; Agrawal, R.; Hillhouse, H. W. *Nano Lett.* **2008**, *8*, 2982–2987.
(3) Tang, J.; Hinds, S.; Kelley, S. O.; Sargent, E. H. *Chem. Mater.* **2008**, *20*, 6906–6910.
(4) Todorov, T.; Cordoncillo, E.; Sanchez-Royo, J. F.; Carda, J.; Escribano, P. *Chem. Mater.* **2006**, *18*, 3145–3150.
(5) Ahn, S. J.; Kim, K.; Yoon, K. *Curr. Appl. Phys.* **2008**, *8*, 766–769.
(6) Repins, I.; Contreras, M. A.; Egaas, B.; DeHart, C.; Scharf, J.; Perkins, C. L.; To, B.; Noufi, R. *Prog. Photovoltaics: Res. Appl.* **2008**, *16*, 235–239.
(7) Cahen, D.; Dagan, G.; Mirovsky, Y.; Hodes, G.; Giriat, W.; Lubke, M. *J. Electrochem. Soc.* **1985**, *132*, 1062.
(8) Pan, D.; An, L.; Sun, Z.; Hou, W.; Yang, Y.; Yang, Z.; Lu, Y. *J. Am. Chem. Soc.* **2008**, *130*, 5620–5621.
(9) Kuo, K.-T.; Chen, S.-Y.; Cheng, B.-M.; Lin, C.-C. *Thin Solid Films* **2008**, *517*, 1257–1261.
(10) Kino, T.; Kuzuya, T.; Itoh, K.; Sumiyama, K.; Wakamatsu, T.; Ishidate, M. *Mater. Trans.* **2008**, *49*, 435–438.
(11) Nairn, J. J.; Shapiro, P. J.; Twamley, B.; Pounds, T.; Von Wandruska, R.; Fletcher, T. R.; Williams, M.; Wang, C. M.; Norton, M. G. *Nano Lett.* **2006**, *6*, 1218–1223.
(12) Zhong, H.; Li, Y.; Ye, M.; Zhu, Z.; Zhou, Y.; Yang, C.; Li, Y. *Nanotechnology* **2007**, *18*, 025602.
(13) Zhong, H.; Zhou, Y.; Ye, M.; He, Y.; Ye, J.; He, C.; Yang, C.; Li, Y. *Chem. Mater.* **2008**, *20*, 6434–6443.

10.1021/cm900363w CCC: $40.75
Published on Web 04/03/2009

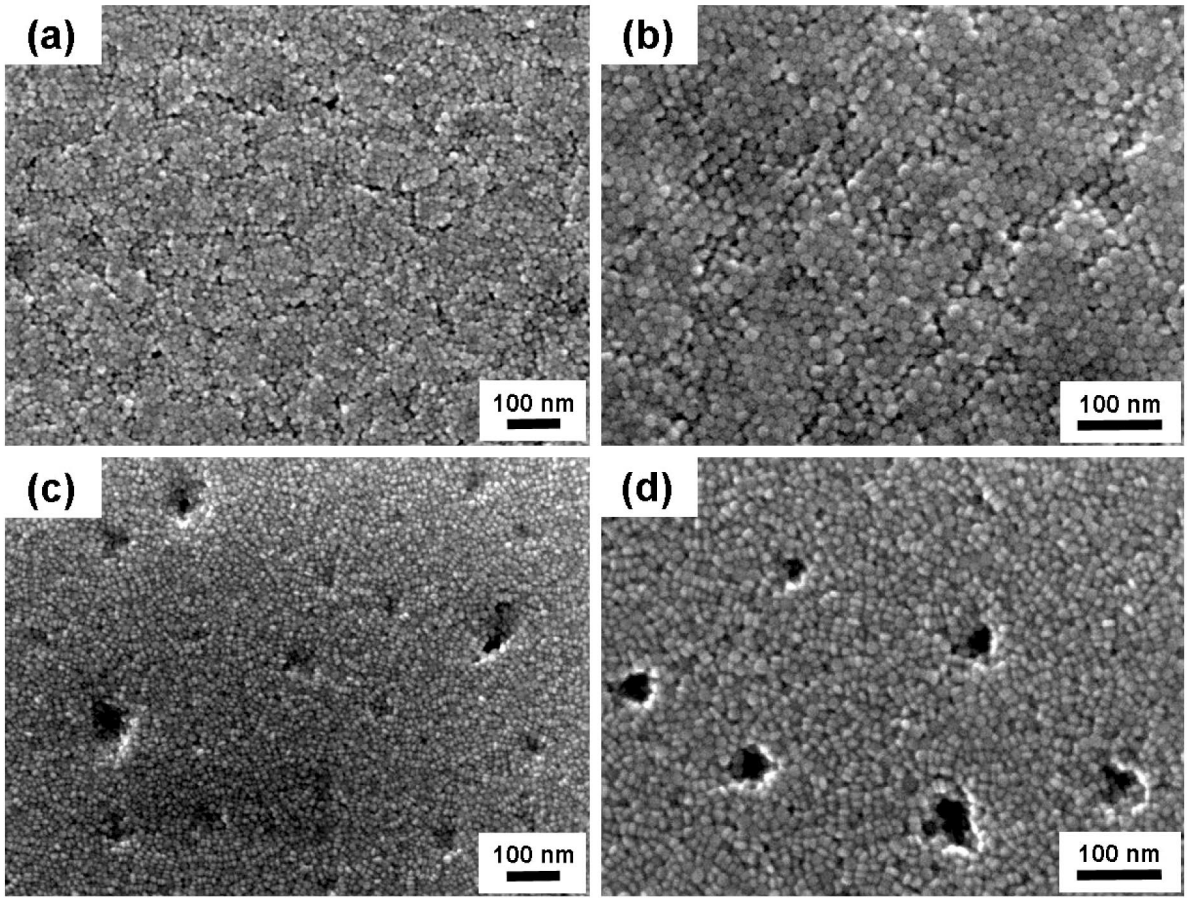

Figure 2. SEM images of $CuInS_2$ nanodisks on silicon substrates coated with either (a,b) native oxide or (c,d) silicon nitride (Si_3N_4). In these two cases, the orientation of the nanodisks is different on the substrates, resting either on their faces as in (a) and (b) or on their sides as in (c) and (d).

positionally disordered cubic, sphalerite. Schimmel et al.[22] has reported the formation of wurtzite $CuInS_2$ by thin film electrodeposition, and coincidentally, Pan et al.[8] also recently observed wurtzite $CuInS_2$ in their colloidally grown nanocrystals. High-resolution transmission electron microscopy (HRTEM) of our $CuInS_2$ nanodisks, however, revealed a significant amount of polytypism with most of the nanodisks having domains of chalcopyrite $CuInS_2$ interfaced with wurtzite $CuInS_2$ across $(002)_w/(112)_{ch}$ stacking faults.[23] This is the first example of wurtzite−chalcopyrite polytypism in a I−III−VI_2 compound and is a consequence of the high surface area to volume ratio of the nanodisks and the colloidal synthesis.

Experimental Details

Chemicals. Copper(I) chloride (CuCl, Aldrich, 99.995+ %), indium(III) chloride ($InCl_3$, Aldrich, 99.999%), copper(II) acetylacetonate ($Cu(acac)_2$, Aldrich, 99.99+%), thiourea (Fluka, •99.0%), and oleylamine (Fluka) were purchased and used as-received.

$CuInS_2$ Nanodisk Synthesis. A mixture of 0.05 g of CuCl (0.5 mmol of Cu), 0.11 g of $InCl_3$ (0.5 mmol of In), 0.076 g of thiourea (1.0 mmol of S), and 10 mL of oleylamine is vigorously stirred (this solution has a dark brown color) and degassed in the reaction flask for 30 min at 60 °C by pulling vacuum on a Schlenk line. The flask is then filled with nitrogen and heated to 240 °C at a rate of 15 °C/min. During the heating process, smoke begins to evolve at about 200 °C and the color turns a darker color, indicating nanocrystal nucleation and growth. After the reaction is allowed to proceed for 1 h, the reaction flask is removed from the heating mantle and allowed to cool to room temperature. Thirty milliliters of ethanol is then added to precipitate the nanocrystals, followed by centrifugation at 7000 rpm for 3 min. The supernatant is discarded. The nanocrystals redisperse in a variety of nonpolar organic solvents, including chloroform, hexane, and toluene. Prior to characterization, dispersions are centrifuged again at 6000 rpm for 1 min to remove inadequately capped nanocrystals. A typical reaction yields approximately 200 mg of $CuInS_2$ nanocrystals.

Materials Characterization. Nanocrystals were imaged by scanning and transmission electron microscopy (SEM and TEM).

(14) Castro, S. L.; Bailey, S. G.; Raffaelle, R. P.; Banger, K. K.; Hepp, A. F. *Chem. Mater.* **2003**, *15*, 3142–3147.
(15) Nakamura, H.; Kato, W.; Uehara, M.; Nose, K.; Omata, T.; Otsuka-Yao-Matsuo, S.; Miyazaki, M.; Maeda, H. *Chem. Mater.* **2006**, *18*, 3330–3335.
(16) Uehara, M.; Watanabe, K.; Tajiri, Y.; Nakamura, H.; Maeda, H. *J. Chem. Phys.* **2008**, *129*, 134709.
(17) Wang, D.; Zheng, W.; Hao, C.; Peng, Q.; Li, Y. *Chem. Commun.* **2008**, 2556–2558.
(18) Du, W.; Qian, X.; Yin, J.; Gong, Q. *Chem.−Eur. J.* **2007**, *13*, 8840–8846.
(19) Dutta, D. P.; Sharma, G. *Mater. Lett.* **2006**, *60*, 2395–2398.
(20) Koo, B.; Patel, R. N.; Korgel, B. A. *J. Am. Chem. Soc.* **2009**, *131*, 3134–3135.
(21) Wurtzite $CuInS_2$ is not stable relative to the cubic (chalcopyrite) phase in the bulk. Binsma, J. J. M.; Giling, L. J.; Bloem, J. *J. Cryst. Growth* **1980**, *50*, 429.
(22) Schimmel, M. I.; de Tacconi, N. R.; Rajeshwar, K. *J. Electroanal. Chem.* **1998**, *453*, 187–195.
(23) The subscripts "w" and "ch" indicate the corresponding "wurtzite" and "chalcopyrite" lattice planes at the stacking fault.

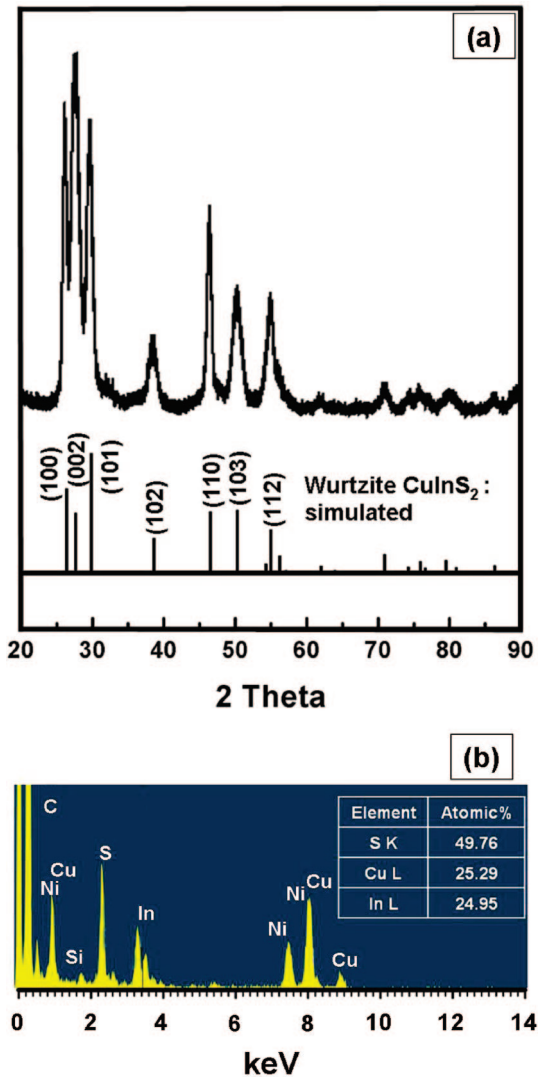

Figure 3. (a) XRD and (b) EDS of $CuInS_2$ nanodisks. The stick patterns for wurtzite $CuInS_2$ shown in (a) were calculated with the CaRIne Crystallography 3.1 program using the following lattice parameters: space group, *P*63*mc* (No. 186) and unit cell dimensions $a = b = 3.897(3)$ Å and $c = 6.441(0)$ Å).[8] The Ni, C, and Si signals in the EDS data are from the nickel grid, the carbon support, and the background in the TEM. Additional EDS data obtained from individual $CuInS_2$ nanodisks is provided in the Supporting Information.

TEM images were acquired on a JEOL 2010F microscope equipped with a field emission gun operated at 200 kV. TEM samples were prepared by drop-casting from chloroform dispersions onto carbon-coated Ni TEM grids (200 mesh, Electron Microscopy Sciences). The JEOL 2010F has an Oxford X-ray energy dispersive spectroscopy (EDS) detector, which was used for elemental analysis. SEM images were acquired with a Zeiss Supra 40 VP SEM at a working voltage of 10−15 kV and working distance of 6 mm.

XRD patterns were obtained from nanocrystal films that were approximately 200 μm thick on quartz substrates. A Bruker-Nonius D8 Advance powder diffractometer with Cu Kα radiation (λ = 1.54 Å) was used with a scan rate of 6°/min in 0.01° increments, collecting for 12 h with that sample rotating at 15°/min.

Room temperature UV−visible absorbance spectra were collected on a Varian Cary 5000 Scan spectrophotometer with samples dispersed in chloroform in quartz cuvettes.

(24) Tell, B.; Shay, J. L.; Kasper, H. M. *Phys. Rev. B* **1971**, *4*, 2463–2471.

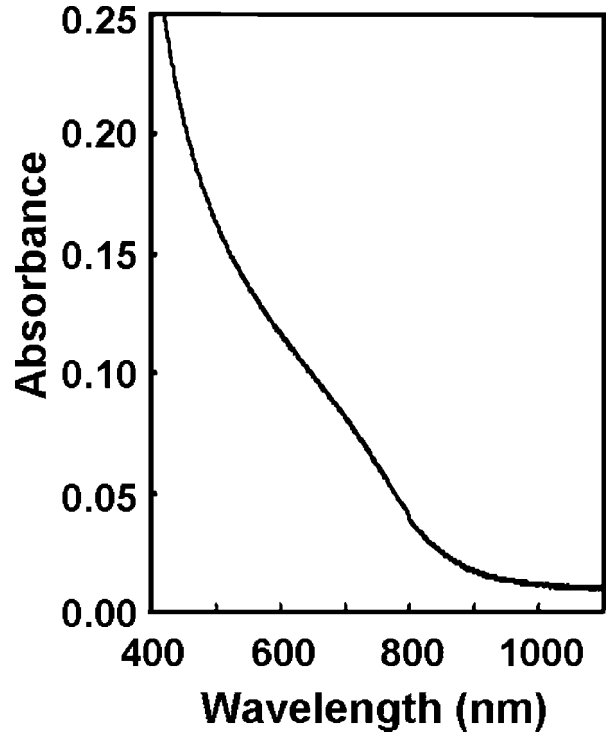

Figure 4. Room temperature UV−vis absorbance spectra of an optically clear dispersion of $CuInS_2$ nanocrystals in chloroform. The absorption edge corresponds to an optical gap of 1.53 eV, which is consistent with bulk $CuInS_2$.

Results and Discussion

Figures 1 and 2 show TEM and SEM images of the $CuInS_2$ nanodisks synthesized by heating CuCl, $InCl_3$, and thiourea in oleylamine at 240 °C. The nanodisks are monodisperse with average diameter and thickness of 13.4 and 5.7 nm. The standard deviation about the mean diameter is ±12.0%. The disk shape of the particles is easily observed, as they either deposit flat with their faces on the substrate or on their sides, in some cases stacking face-to-face into columns extended parallel to the substrate (see for example Figures 1c, 2c, and 2d). EDS (Figure 3b) confirmed that the nanodisks are composed of $CuInS_2$, with Cu:In:S atomic ratios very near 1:1:2. The optical absorption edge in the UV−vis absorbance spectra also corresponds to the expected band gap energy of 1.53 eV typical of bulk $CuInS_2$ (Figure 4).[24]

The XRD patterns (Figure 3a) from the nanodisks, however, were characteristic of a hexagonal wurtzite structure as opposed to the expected tetragonal chalcopyrite structure. Although the wurtzite phase was unexpected, Pan et al.[8] also recently observed the formation of wurtzite $CuInS_2$ nanocrystals. The XRD pattern calculated using the lattice parameters reported by Pan et al.[8] (space group: *P*63*mc* (No. 186) and unit cell dimensions $a = b = 3.897(3)$ Å, $c = 6.441(0)$ Å) gave a good match to the experimental diffraction pattern, as shown in Figure 3a. (See Supporting Information for a comparison of the XRD patterns to other possible phases.)

The nanodisks were further studied by high-resolution TEM. Figure 5 shows TEM images of the nanodisks with two different orientations on the substrate. The FFT of the image in Figure 5a corresponds to a crystal with a hexagonal structure with the nanodisk being viewed down the [001]

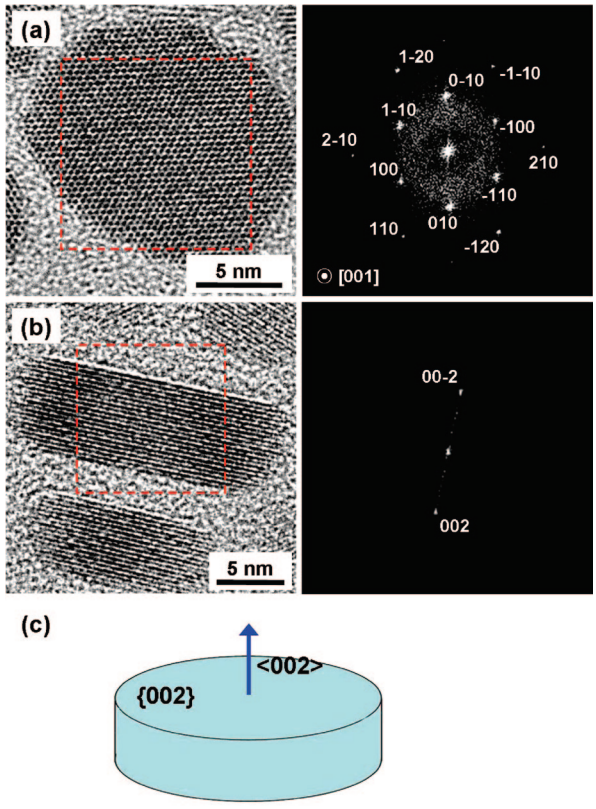

Figure 5. TEM images of $CuInS_2$ nanodisks with two different orientations on the substrate: (a) lying flat and (b) standing on edge. The FFTs are consistent with wurtzite $CuInS_2$: the (100) spots do not appear in the chalcopyrite structure. (c) Illustration of the crystallographic orientation of the nanodisks based on TEM images like those in (a) and (b).

zone axis (i.e., the *c*-axis of the wurtzite $CuInS_2$ crystal structure). The top and bottom faces of the disk are bounded by {002} planes, as illustrated in Figure 5c. Similar crystallographic orientations have been observed for CuS and Cu_2S nanodisks with hexagonal crystal structure.[25,26]

But extensive TEM revealed that a significant amount of chalcopyrite $CuInS_2$ was also present in the nanodisks. We noticed that stacking faults were present in many nanodisks imaged on their sides. A careful structural analysis of the TEM images showed that part of the crystal was actually in the chalcopyrite phase. This was surprising because XRD quite clearly showed that the nanodisks were composed of wurtzite $CuInS_2$. But a more careful look at the XRD peak intensities also revealed that wurtzite−chalcopyrite polytypism was present in the sample. The diffraction peak positions matched wurtzite $CuInS_2$, but the intensities of the peaks corresponding to chalcopyrite—i.e., the wurtzite (002), (110), and (112) peaks—were slightly higher than expected. Most nanodisks turned out to have crystalline wurtzite domains interfaced with chalcopyrite domains across $(002)_w/(112)_{ch}$ stacking faults, like the nanodisk in Figure 6.

The crystal phase of the nanodisks is therefore most accurately described as *polytypic*, as both wurtzite and chalcopyrite crystal domains coexist within each nanodisk. For example, the FFT in Figure 6b generated from the crystalline region outlined by the red square in (a) has more

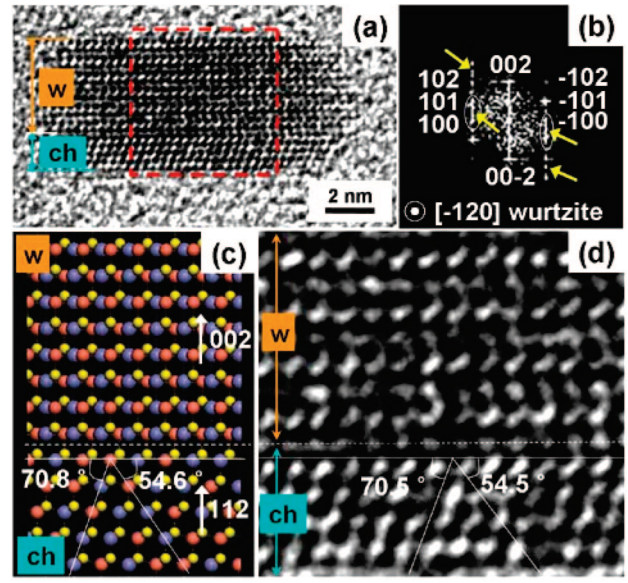

Figure 6. (a) HRTEM image of the $CuInS_2$ nanocrystal with [$\bar{1}$20] zone axis and (b) FFT of the red square area in (a). The FFT shows multiple diffraction spots (indicated by yellow arrows) from chalcopyrite structure at the lower part. (c) A crystal model showing the {$\bar{1}$20} wurtzite plane and its equivalent {0$\bar{2}$4} chalcopyrite plane. The crystal models were generated using Materials Studio and the angles between lattice planes were calculated by CaRIne Crystallography 3.1 program. (d) Magnified image of the region bordered by the red square in (a) with the same scale as the simulated crystal in (c). ("w" and "ch" indicate wurtzite and chalcopyrite, respectively.)

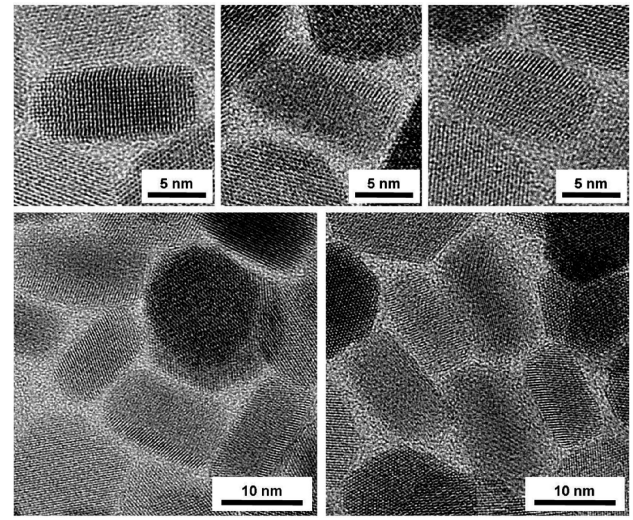

Figure 7. HRTEM images of $CuInS_2$ nanodisks oriented on their sides, exhibiting wurtzite−chalcopyrite polytypism.

spots (indicated by the yellow arrows) than expected for a wurtzite crystal imaged down the [$\bar{1}$20] zone axis. These additional spots arise from the change in crystal structure to chalcopyrite across the stacking fault. Figure 7 shows additional TEM images of polytypic nanodisks and Figure 8 shows another example of a nanodisk imaged on its side and the FFTs generated from different positions of the crystal showing the wurtzite−chalcopyrite polytypism.

It should be appreciated that the wurtzite−chalcopyrite polytypism can be observed only in TEM images of nanodisks with particular orientations on the substrate. For example, nanodisks oriented on their faces (like the one

(25) Ghezelbash, A.; Korgel, B. A. *Langmuir* **2005**, *21*, 9451–9456.
(26) Sigman, M. B.; Ghezelbash, A.; Hanrath, T.; Saunders, A. E.; Lee, F.; Korgel, B. A. *J. Am. Chem. Soc.* **2003**, *125*, 16050–16057.

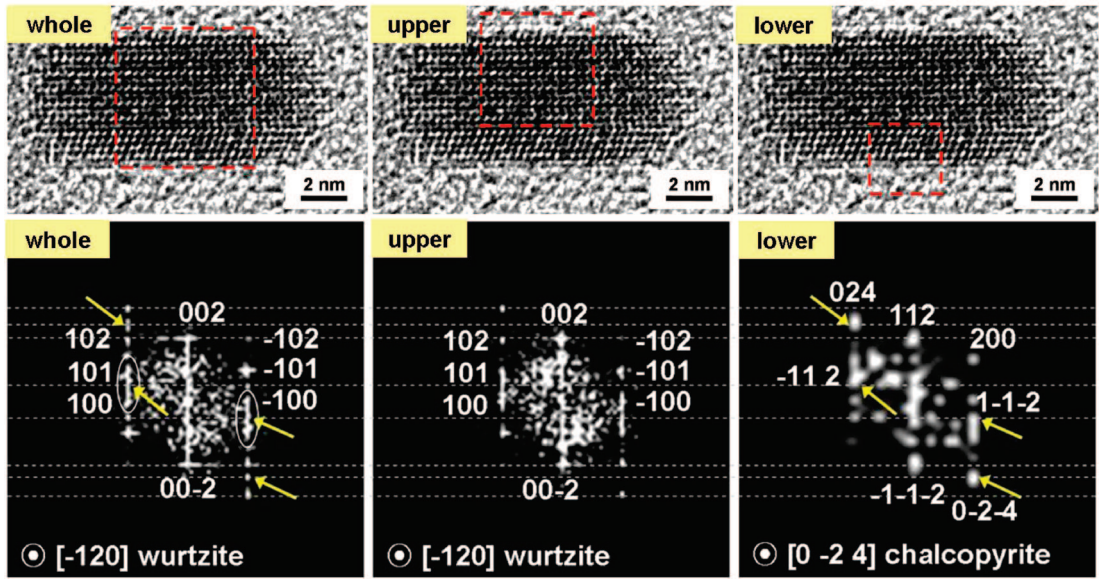

Figure 8. FFTs generated from a TEM image of a $CuInS_2$ nanodisk in the different regions of the crystal outlined in red. The additional spots in the FFT arise from the crystalline chalcopyrite domain ([$0\bar{2}4$] zone axis), indicated by yellow arrows under the wurtzite domain.

imaged in Figure 5a) and imaged down the $[001]_w$ zone axis appear to be single crystals as the $(002)_w/(112)_{ch}$ stacking faults within the interior of the nanodisk are not visible when viewed in this crystallographic direction. The stacking faults are observable only when the crystal is imaged down the $[\bar{1}20]_w$ zone axis.

Conclusions

A new synthetic route was developed that produced monodisperse $CuInS_2$ nanodisks. The nanodisks exhibited wurtzite−chalcopyrite polytypism with the coexistence of both wurtzite and chalcopyrite domains interface across $(002)_w/(112)_{ch}$ stacking faults. This is the first example of wurtzite−chalcopyrite polytypism in I−III−VI_2 compounds that we are aware of. The phase behavior and crystal structure of nanocrystalline materials are known to differ in some cases from bulk materials, as in the case of Co nanocrystals with an unusual ϵ-phase,[27−29] $AgInSe_2$ nanorods with a new orthorhombic phase,[30] and $CuInS_2$ with an unexpected wurtzite phase.[8] The wurtzite−chalcopyrite polytypism observed here for $CuInS_2$ nanodisks provides another example of unexpected phase behavior. Another important feature of nanocrystals is their ability to accommodate significant amounts of lattice strain at interfaces, which leads to different defect formation mechanisms than in bulk materials,[31−34] and may provide another reason why these nanodisks exhibit wurtzite−chalcopyrite polytypism that is uncommon in bulk or thin film materials.

Acknowledgment. This research was supported by funding from the National Science Foundation through their STC program (CHE-9876674), the Robert A. Welch Foundation, and the Air Force Research Laboratory (FA8650-07-2-5061).

Supporting Information Available: Additional EDS data of $CuInS_2$ nanodisks, XRD pattern analysis, and supplementary experimental data (TEM, HRTEM, and XRD). This material is available free of charge via the Internet at http://pubs.acs.org.

CM900363W

(27) Sun, S.; Murray, C. B. *J. Appl. Phys.* **1999**, *85*, 4325–4330.
(28) Dinega, D. P.; Bawendi, M. G. *Angew. Chem., Int. Ed.* **1999**, *38*, 1788–1791.
(29) Puntes, V. F.; Krishnan, K. M.; Alivisatos, A. P. *Science* **2001**, *291*, 2115–2117.
(30) Ng, M. T.; Boothroyd, C. B.; Vittal, J. J. *J. Am. Chem. Soc.* **2006**, *128*, 7118–7119.
(31) Kamalov, V. F.; Little, R.; Logunov, S. L.; El-Sayed, M. A. *J. Phys. Chem.* **1996**, *100*, 6381–6384.
(32) Chen, X.; Lou, Y.; Samia, A. C.; Burda, C. *Nano Lett.* **2003**, *3*, 799.
(33) Shenoy, V. B. *Phys. Rev. B* **2005**, *71*, 094104.
(34) Koo, B.; Korgel, B. A. *Nano Lett.* **2008**, *8*, 2490–2496.